Quasi-Optical Planar Arrays with FET's and Slots

Shigeo Kawasaki and Tatsuo Itoh, *Fellow, IEEE*

Abstract— **This paper describes the design concept and the experimental results of prototypes of two-dimensional quasi-optical power combining arrays. Several different quasi-optical circuits were made to obtain the fundamental data for this study. How to incorporate the antenna input impedance into the active antenna circuit and how to analyze the strong coupling condition with two operation modes are addressed by using a large signal analysis. Several configurations of the circuits are demonstrated, such as a single active antenna operating at 9.3 GHZ and 24.0 GHZ, a 6-element linear power combining array operating at 15.6 GHZ and 4-element and 16-element two-dimensional power combining arrays operating at 10.4 GHz and 7.8 GHz. Important characteristics such as antenna patterns and tuning ranges are discussed. Finally, the prospects for a two-dimensional monolithic quasi-optical power combining array are discussed.**

I. Introduction

OVER THE past several years, radio engineers have discovered a need to create new forms of active circuits which consist of passive antenna elements and active semiconductor devices, and operate at high frequencies. More compact radars are required for military purposes, while light-weight and low-cost transceivers are essential for space and personal communication. Due to these requirements, the development of new components and new ways of implementing the components are necessary. The quasi-optical and active antenna technology have been created to satisfy these requirements.

The significant feature of the quasi-optical or active antenna circuit is not to simply combine antennas with solid state devices through transmission lines, but to provide circuit characteristics resulting from antenna characteristics to form an integrated circuit antenna as a single entity [1]. Therefore, the circuit is integrated with appropriate radiating elements and solid state devices so that their interactions are taken into account from the outset of the design.

Quasi-optical power combiners depending on their locking methods may be divided into two types; the wave-beam type and the array type. The concept of the wave-beam type combiner [2] has been realized by a distributed grid oscillator using the Fabry–Perot resonator [3]. On the other hand, the features of the array type combiner are a planar or layered structure. Further, in this type of combiner, the spacing between two adjacent radiators plays an important role for high power generation. The array type combiner is divided into two categories; the external injection locking type [4] and the internal mutual coupling type. The internal mutual coupling combiners can be further subdivided into two types; a combiner by utilizing the mutual coupling between antennas, which may be enhanced by reflection from a dielectric back plate (weak coupling) [5], and a combiner due to coupling the RF signal generated from active sources through the direct connection with a transmission line (strong coupling) [6]. In the strongly coupled combiner, the RF energy travels to adjacent active sources. Hence, the phase relationship among outputs of the active sources should be taken into consideration in the design in order to effectively combine the powers radiated from the antennas [7].

Although several planar antennas can be used for quasi-optical application, the slot antenna is extensively used in this paper. A slot radiator in the circuit ground plane increases design flexibility since both sides of the substrate can be effectively used [8]. As a result, the structures for the antenna part and the circuit part are stratified. The slot is electromagnetically coupled through a microstrip-to-slot line transmission which is easily designed into the layered structure.

In this paper, several examples are given for active antennas and quasi-optical planar arrays with strong coupling. The radiating elements are slots in the ground plane, and the active devices are negative resistance FET's. For analysis, the slot input impedance is included in the circuit model not only to simulate the input impedance of the passive part of the quasi-optical circuit but to investigate a steady state oscillation status using a large signal analysis. The operating frequencies predicted from the passive part analysis and from the large signal analysis agree with experimental results with less than 10% error.

II. Design

When we design an active antenna and a quasi-optical power combining array with strong coupling, the following three factors are important; impedance matching at a branching point, the phase of the radiating signal on the slot, and the signal phase from the oscillator. These items are incorporated in the design of each circuit as discussed below. Since the input impedance of the slot antenna needs to be included in the design of the quasi-optical oscillator circuit, an evaluation and a simple expression are provided in the Appendix.

1. Active Antenna with Single FET Oscillator and Single Slot and Linear Quasi-Optical Power Combining Array

A. Layered Active Antenna with Single FET and Single Slot

The simplest way to realize the single active antenna is to design an oscillator circuit with one or more radiation ele-

Manuscript received September 11, 1992; revised March 12, 1993. This work was supported by the U.S. Army Research Office under Contract DAAL 03-88-K-0005.

The authors are with UCLA, Electrical Engineering Department, Los Angeles, CA 90024-1594

IEEE Log Number 9211939.

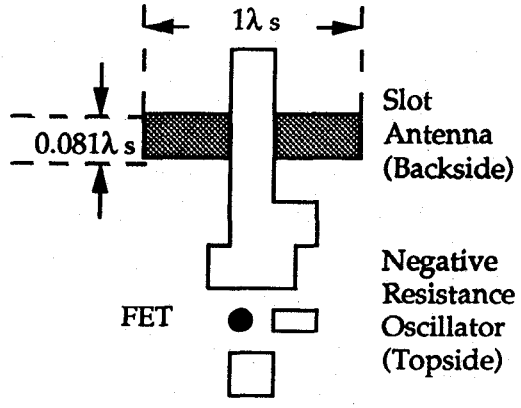

Fig. 1. Configuration of active antenna with single FET and single slot.

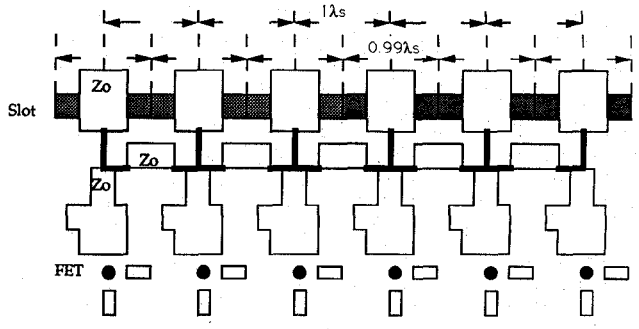

Fig. 2. Configuration of 6-element periodic linear power combining array.

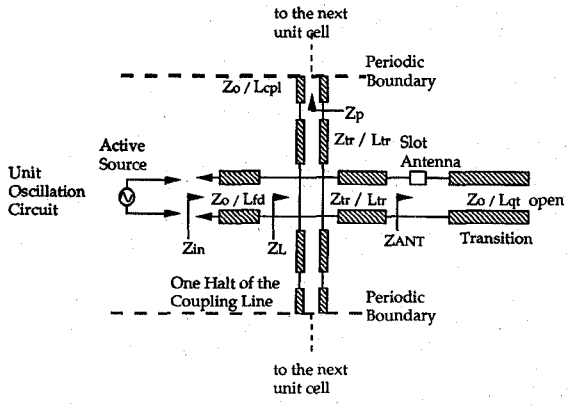

Fig. 3. Unit-cell of periodic quasi-optical power combining array.

ments. A single oscillator with a single radiator is considered as the unit-cell of a quasi-optical power combining array. Fig. 1 shows the single active antenna with a slot radiator in the ground plane. The advantage of this configuration is that undesired radiation from the circuit part is eliminated when the antenna pattern is measured in the ground plane side. The slot length is $1\lambda_s$ and the slot width is $0.081\lambda_s$ (where λ_s is the guided slot wavelength). This slot dimension will be used in all circuits reported in this paper except a linear array (the slot length is $0.99\lambda_s$). The negative resistance value of the FET oscillator was designed as $-50\ \Omega$ using small signal S-parameters. In order to constitute the layered structure, a quarter wavelength open-end circuit with a characteristic impedance, Z_o, of 50 Ω is used as a microstrip-to-slot line transition. Through this transition, the slot antenna which is electromagnetically coupled with the microstrip line provides an appropriate load to the active device. By altering the length of this open-end circuit, the oscillation frequency can be tuned. In this case, the open-end circuit works as a tuning stub which cancels the reactance of both the antenna input impedance and the drain output impedance of the FET.

B. Linear Quasi-Optical Power Combining Array

Using the active antenna described above, a linear quasi-optical power combining array with six unit-cells was designed. The circuit configuration is shown in Fig. 2. Six slot radiators are aligned in the H-plane. In order to increase the packing density, the distance between the centers of the two adjacent slots is $0.77\lambda_{of}$ (where λ_{of} is the design wavelength in free space). To invoke a strong coupling, transmission lines are used to connect not only the oscillators with the antennas but also adjacent oscillators together. Therefore, for analysis, we can assume that the dominant coupling of the quasi-optical power combing array is through the transmission line, and the mutual coupling of the antennas can be neglected. Since the circuit has a periodicity, the analysis and design can be simplified by assuming an ideal oscillator and by applying a periodic boundary condition. Based on this argument, we can show a reduced unit-cell model for the periodic quasi-optical power combining array as shown in Fig. 3.

To obtain the in-phase radiating signal from each oscillator, we must adjust the length of the coupling line and the reflection coefficient of the FET oscillator. If the length of the coupling line is $\lambda/2$ and an argument of the reflection coefficient is π, the signal phase from each oscillator is in-phase. This is because a phase progress along the coupling line is π and a phase progress of an injected and reflected signal is also π, therefore, a total phase progress of the signal is 2π. As a result, the in-phase signal transmitted toward radiators is expected. If the coupling line is λ, the argument of the reflection coefficient should be 2π according to the similar argument discussed above.

Due to the combination of many active sources, it is possible that the combiner has many modes. Of these modes, the in-phase mode and the anti-phase mode are very important for the antenna pattern as well as combining efficiency. In particular, the in-phase mode is desired for high combining efficiency in the broadside direction. Since these modes are dependent upon the loading seen by the active devices, it is important to investigate the input impedance of the passive part of the array. In the periodic structure, a field maximum joint (open-circuit status) is at the periodic boundary for the in-phase mode, while a minimum field point (short-circuit status) is there for the anti-phase mode. Characteristic impedances and lengths of transmission lines required for analysis are given in Fig. 3. Using the ABCD matrix, the input impedance of this circuit is

$$Z_{\text{in}} = Z_o \frac{1 + jy_L \tan \beta L_{fd}}{y_L + j \tan \beta L_{fd}}$$

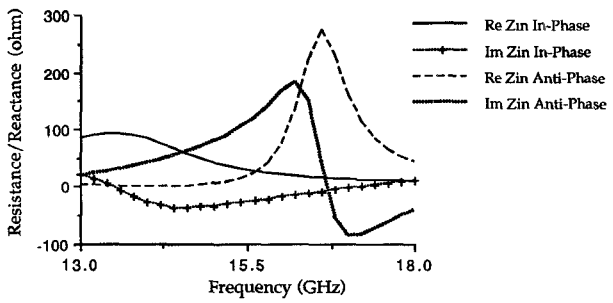

Fig. 4. Input impedance variation of unit-cell model for two modes.

TABLE I
PARAMETERS OF INPUT IMPEDANCES OF PASSIVE PART

	In-Phase (open)	Anti-Phase (short)
fo (resonant frequency)	17.2 GHz	16.7 GHz
$\mathrm{Re}\{Z_{\mathrm{in}}\}$	12.4 Ω	251 Ω
$\mathrm{Im}\{Z_{\mathrm{in}}\}$	1.0 Ω	−3.9 Ω

where

$$y_L = \frac{Z_o}{Z_L} = \frac{Z_o}{Z_{tr}} \cdot \left\{ \frac{Z_{ANT} j \tan \beta L_{tr} + Z_{tr}}{Z_{ANT} + j Z_{tr} \tan \beta L_{tr}} + \frac{2(Z_p j \tan \beta L_{tr} + Z_{tr})}{Z + j Z_{tr} \tan \beta L_{tr}} \right\}$$

$$Z_p \begin{cases} = \dfrac{Z_{cpl}}{j \tan \beta L_{cpl}} & \text{(In-phase Mode)} \\ = Z_{cpl} j \tan \beta L_{cpl} & \text{(Anti-phase Mode)} \end{cases}$$

As an example, let us study the variation of Z_{in}, under the conditions of f_o (the design frequency) = 16 GHz, $Z_o = Z_{cpl} = 50\ \Omega$, $Z_{tr} = 86.6\ \Omega$, and $L_{fd} = 0.1\ \lambda_{om}$ (where λ_{om} is the guided wavelength in the microstrip line at the design frequency). Fig. 4 shows frequency characteristics of Z_{in}. Each parameter is indicated in Table I. If an equivalent circuit of the active source is denoted by a series resistance and a reactance, the resistance degrades in the steady state oscillation. Since the active source is designed at $-50\ \Omega$, the circuit resistance must be less than 50 Ω. Therefore, the circuit can have the in-phase mode at 17.2 GHz, and the anti-phase mode is suppressed because it sees a high resistance shown in Table I.

Another method to predict an operating frequency is to use a large signal analysis. For this purpose, a commercially available harmonic balance analysis (Libra by EEsof) was used. In this case, an active part was combined with the passive part shown in Fig. 3. The simulation results for the two modes are shown in Fig. 5. From these results, it is found that only the in-phase mode can grow and its operating frequency is 16.3 GHz. This value is 4% lower than the operating frequency from the passive part analysis indicated in Table I.

According to the argument above, we can propose a new technique to invoke a desired mode in the design of a quasi-optical power combining array with strong coupling. Namely, a half of the coupling line in a reduced unit-cell model can be replaced with an appropriate stub for the desired mode (an open stub for the in-phase mode or a short stub for the anti-phase mode). This design technique is useful for an array with a periodic structure.

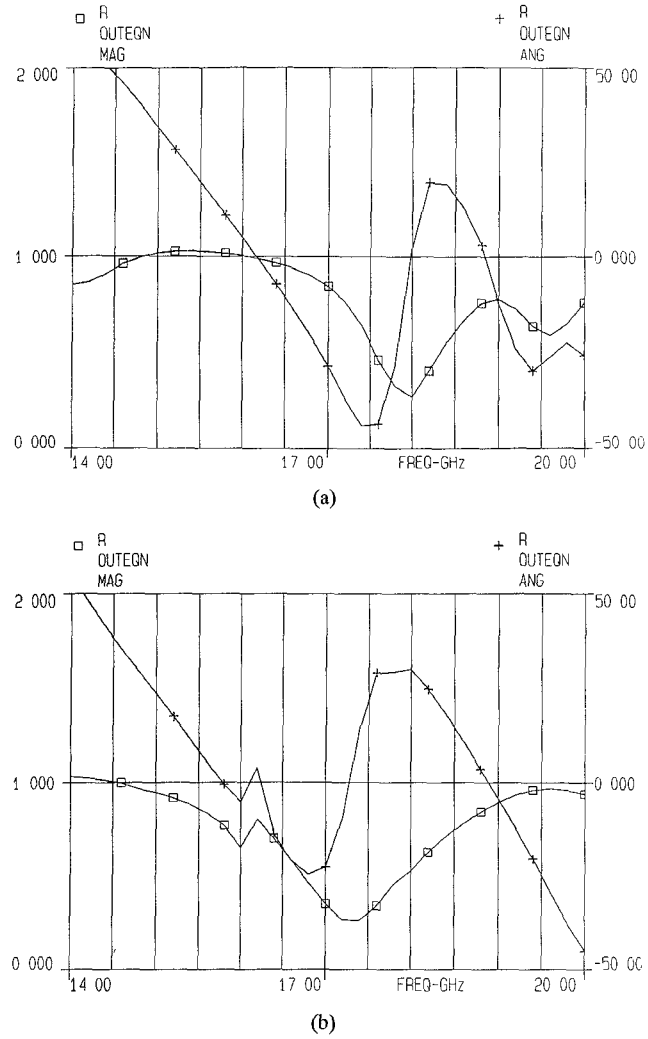

Fig. 5. Large signal analysis of unit-cell of 6-element array. (a) In-phase case. (b) Anti-phase case.

2. Active Antenna with Single FET Oscillator and Multislots and Two-Dimensional Quasi-Optical Power Combining Array

A. Layered Active Antenna with Single FET and Four Slots

An active antenna with a single FET oscillator and four slots was fabricated in a hybrid form as shown in Fig. 6. An advantage of this oscillator is the increase of the receiving power density in the broadside direction using the same source power. For instance, in the case of a N-slot array, RF energy generated from the oscillator is divided into $1/N$ by a power divider and the energy is delivered to each slot. Ideally, a radiating field is proportional to $1/\sqrt{N}$. When the radiations from the four slots are combined in the broadside direction, the total field at the front of a receiving antenna is proportional to $\sqrt{N}(= N/\sqrt{N})$. Then, the receiving power has a factor of N compared with that in a single slot case.

The circuit shown in Fig. 6 was designed at 10 GHz to be able to radiate dual orthogonal linear polarized waves (in short, dual polarized waves). At Point A, four branches are

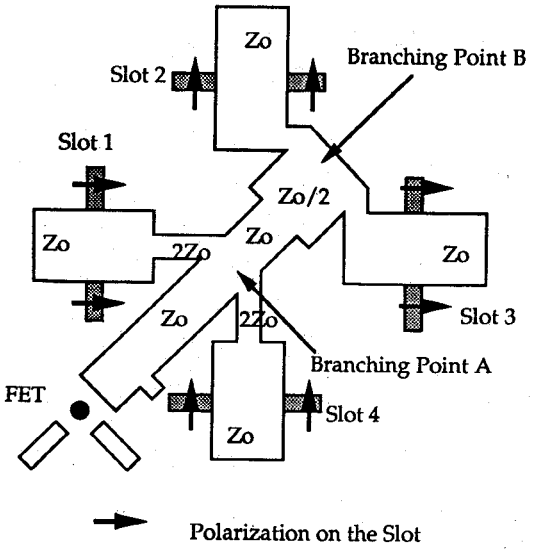

Fig. 6. Configuration of active antenna with single FET and four slots.

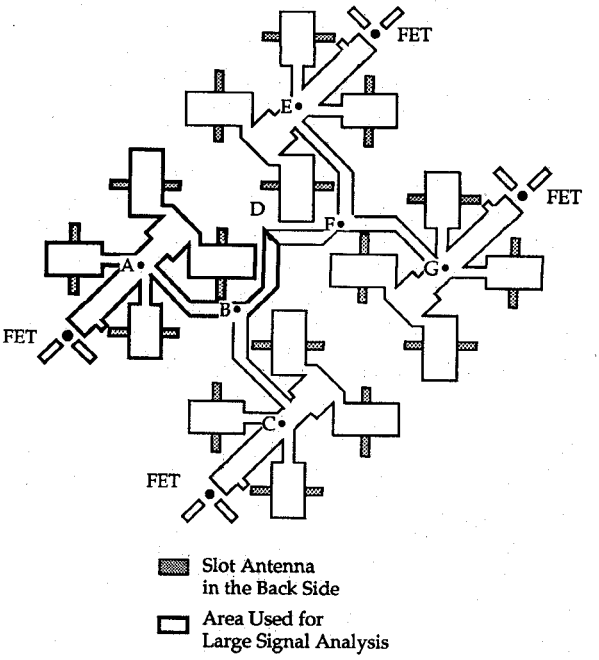

Fig. 7. Two-dimensional power combining array.

connected. One branch with a characteristic impedance Z_o is connected to the oscillator. Three others are connected to the four antennas via a one stage quarter wavelength transformer used for impedance matching to divide RF energy into the four slots equally. If all feed lines to the slots from Point A had the same electrical lengths, the phase difference of radiation waves between a pair of slots which are sited at the opposite positions with respect to Point A becomes 180 degrees. This results in a difference antenna pattern. In order to create in-phase radiation, an extra transmission line with a half wavelength should be added to only one of the two microstrip feed lines which connect a pair of the slots. In Fig. 6, the upper half lines which lead to Slot 2 and Slot 3 including Point B has the extra transmission line to invert the phase of one of the pair (in this case, Slot 2 with respect to Slot 4 and Slot 3 with respect to Slot 1). Since a pair of the slots sited at the opposite points are now in-phase, we can expect that the circuit radiates a sum antenna pattern in the E-plane. In this circuit, a spacing between a pair of the slots is 1.2 λ_{of}. Therefore, the antenna pattern in the E-plane is expected to include a grating lobe. However, the problem of the grating lobe is resolved by use of a substrate with a much higher permittivity, since the physical length of 1 λ_{om} becomes much smaller.

B. Two-Dimensional Quasi-Optical Power Combining Array

As shown in Fig. 7, a two-dimensional quasi-optical power combining array with four FET oscillators with 16 slots was designed at 10 GHz. This array radiates dual polarizations. As described in the early part of this section, we must consider the following three factors; the impedance matching at a branching point, the phase of the radiating signal on the slot, and the signal phase from the oscillator. The impedance matching and the phase condition of the radiating signal on the slot, is identical to those of the active antenna with a single oscillator and four slots. Meanwhile, a shape and a length of coupling lines should be determined to meet the requirement for a separation of each oscillator as well as an electrical length. If each oscillator has the argument of a reflection coefficient of π, the length of the coupling lines between any two branching points should be $(2n-1)\lambda/2$ (where n is an integer). This is based on the reason discussed in the early part of this design section. In the circuit shown in Fig. 7, the electrical length of A-B-C is 2.5 λ_{om} and that of A-B-D-F-E is 3.5 λ_{om}.

Using the similar, reduced model described in the previous section, a large signal analysis can be carried out. A part of the array indicated in Fig. 7 was used for this purpose. An operating frequency of 8.3 GHz was obtained from the simulation.

III. Experimental Results

Based on the design concept mentioned above, we fabricated several quasi-optical circuits. As a PTFE dielectric substrate, RT 5870 of Rogers Corp. was used. It has a thickness of 0.79 mm (31 mil) with 1 oz copper surfaces and a dielectric constant of 2.33. In each circuit, a package type FET was used as an active source. For the active antenna with single slot and the linear power combining array, the FET's used were ATF 26884 of Avantek and NE 32484A of NEC. For the active antenna with four slots and the two-dimensional power combining array, ATF 13284 of Avantek was used. In the circuits tested in this paper, a high impedance microstrip line with a quarter wavelength radial stub and a bonding pad was used as a bias line for the FET drain and gate. The dc voltage was applied through a thin wire connected to the bonding pad. In the power combining arrays, only one bias network was necessary for the drain bias, since we can make use of the coupling line.

1. Active Antenna with Single FET Oscillator and Single Slot and Linear Quasi-Optical Power Combining Array

Antenna patterns measured for active antennas designed at 10 GHz and 25 GHz are shown in Fig. 8. The oscillation

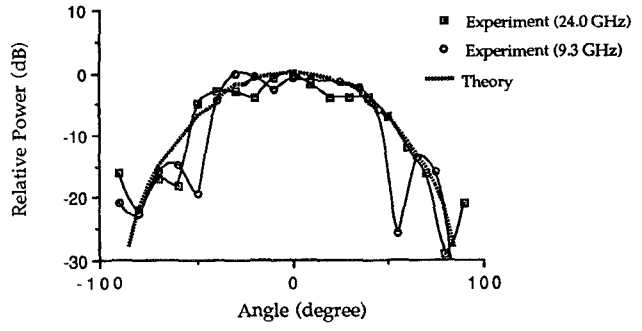

Fig. 8. Antenna pattern comparison for active antenna with single FET and single slot.

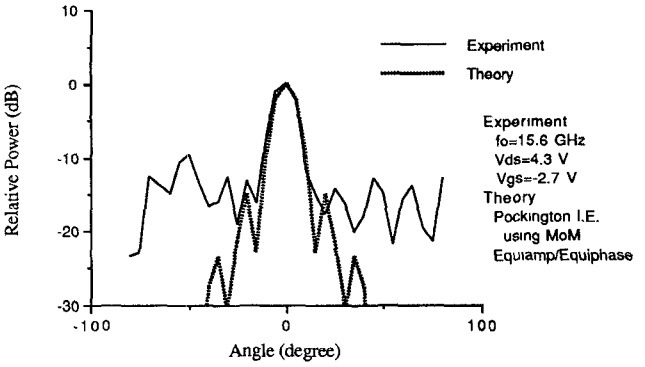

Fig. 9. Antenna pattern comparison for 6-element periodic linear array.

frequencies were 9.3 GHz with $Vds = 3.5$ V and $Vgs = -0.7$ V and 24.0 GHz with $Vds = 3.3$ V and $Vgs = -0.5$ V, respectively. For an active antenna, the Effective Radiated Power (ERP) is defined as the product of isotropic conversation gain [9] and dc bias power. The measured ERP's for the circuits operated at 9.3 GHz and 24.0 GHz were obtained 13.2 dBm and 13.7 dBm, respectively. The tuning ranges due to the change of dc voltages (Vds and Vgs) were 170 MHz and 100 MHz, respectively. In addition, a theoretical antenna pattern calculated from the Pocklington type integral equation and the method of moment is also shown in Fig. 8. Agreement with these three antenna patterns is very good. From these data, it is found that the oscillator design frequency using small signal S-parameters includes less than 7% error and the $1\lambda_s$ slot and the coupling between the oscillator and the slot antenna work well.

For the 6-element periodic linear array, the operating frequency of 15.6 GHz with $Vds = 4.3$ V and $Vgs = -2.7$ V and the tuning range of 58 MHz by changing Vds and Vgs were obtained. The FET used here was ATF 26884. Comparing the experimental operating frequency of 15.6 GHz with the predicted operating frequency of 17.2 GHz from the passive part analysis and of 16.3 GHz from the large signal analysis, the former has 10% error and the latter has 4% error. An antenna pattern and a theoretical pattern are shown in Fig. 9. A sharp main lobe is obvious. Agreement between the theory and the experiment is very good around the main lobe. Compared with a single or a few elements array, the oscillation spectrum was sharp and stable. Perhaps, it is understood that due to a high Q structure with periodicity, undesired modes were suppressed. In any case, the antenna pattern improves as the number of oscillators increases, provided that the circuit can maintain a stable operating condition. Increasing sidelobes resulted from high receiver noise and defects of experimental setup.

2. Active Antenna with Single FET Oscillator and Multislots and Two-dimensional Quasi-Optical Power Combining Array

The operating frequency of the active antenna with four slots was 10.4 GHz with $Vds = 4.2$ V and $Vgs = -0.4$ V. From the measured results, the ERP was estimated as 19.23 dBm. Due to the dual polarizations, an antenna pattern with a horizontal polarization in the horizontal measuring plane is different from that with a vertical polarization in the horizontal measuring plane. As shown in Fig. 10, the former indicates a 2-element array in the E-plane (Fig. 10(a)), while the latter indicates double $1\lambda_s$ slot antennas aligned in a vertical direction (Fig. 10(b)). Therefore, an improved array antenna pattern is expected in the former case, since the E-plane antenna pattern of the slot with a narrow width becomes very broad. On the other hand, a $1\lambda_s$ slot antenna pattern will be observed in the latter case. Fig. 10 shows the measured antenna patterns resulting from this fact. In addition, Theoretical antenna patterns for both cases are also shown in Fig. 10. Agreement between the theory and the experiment is good. Since the distance between the centers of a pair of the slots is 1.2 λ_{of} in the former case (the E-plane 2-element array), the grating lobe is found in the endfire direction.

Fig. 11 shows the measured antenna patterns. The operating frequency was 7.8 GHz with $Vds = 4.23$ V and $Vgs = -0.8$ V. The FET used here was ATF 13284. The operating frequency is lower than the predicted operating frequency of 8.3 GHz from the large signal analysis and is different from the operating frequency of the active antenna with multislots. Perhaps, this is due to impedance mismatch. This mismatch produced interaction of the oscillators such as load pulling. Eventually, this interaction may result in a lower operating frequency. In this case, the distance of the centers of two slots became almost one wavelength of the operating frequency.

The antenna patterns were measured in two ways as described in Fig. 11. The measuring plane is fixed in the horizontal plane. In the case A, the polarization is vertical. Therefore, 8 slots out of 16 slots aligned in the direction along the slot length can contribute to the antenna pattern. The pattern mainly resulting from double 3-element linear slot arrays in the horizontal plane was expected. This explains the obtained pattern for the case A in Fig. 11. Since 8 slots in the E-plane shown in Fig. 11 can contribute to the measurement in the case B, the antenna pattern resulting from the center 4 slots was expected. Due to the narrow slot width, the antenna pattern shows an array factor. In the case B of Fig. 11, this tendency can be seen and a grating lobe was observed.

IV. Conclusions

We have demonstrated several circuits for quasi-optical planar arrays with FET's and slots. We have developed these circuits to provide a step-by-step investigation of quasi-optical

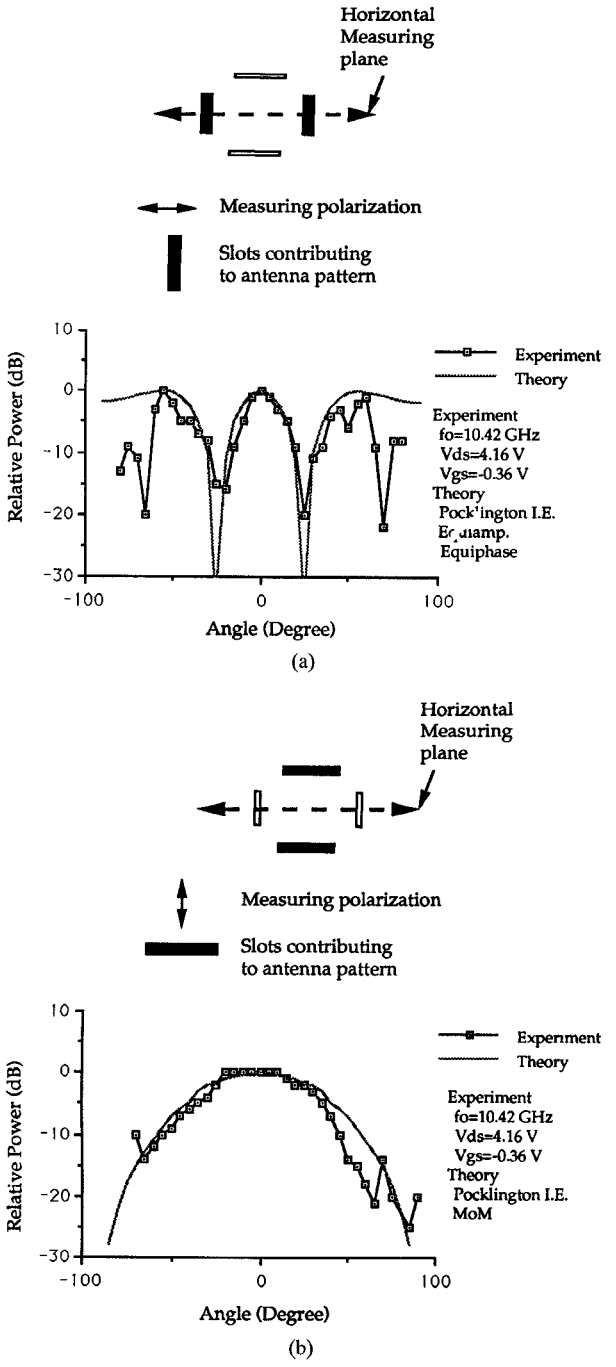

Fig. 10. Antenna pattern comparison for active antenna with single FET and four slot. (a) Measurement case of E-plane z-element array. (b) Measurement case of one wavelength slot antenna.

circuits, in order of increasing complexity from a single planar active antenna to a two-dimensional array. The slot antenna input impedance was included in an entire circuit as a series impedance in a circuit simulation. In addition, the desired mode is incorporated with by replacing a half of the coupling line with an appropriate stub in the design. These design concepts are easily adapted for the monolithic active integrated antenna at higher frequencies. When the MMIC technology is applied to a quasi-optical circuit, it is possible to fabricate a quasi-optical power combining array using a large number of FET oscillators, since the oscillator part becomes very small.

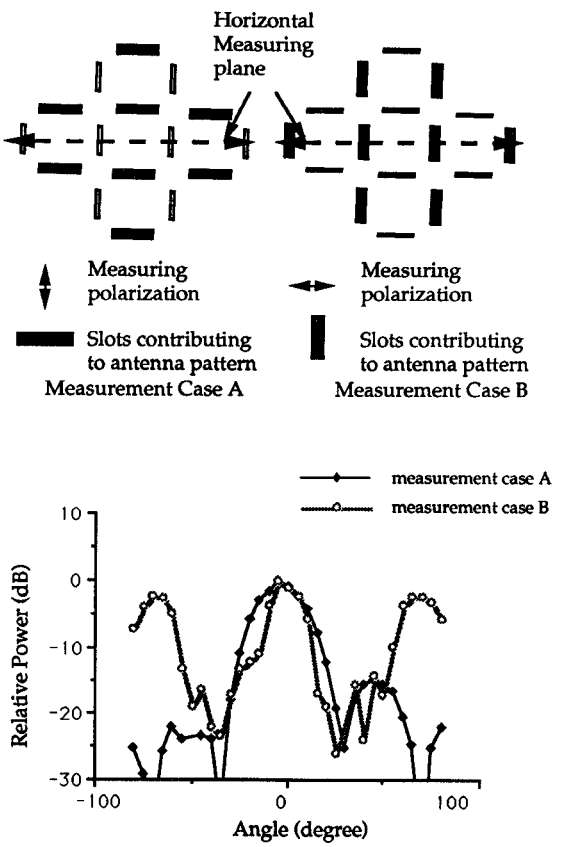

Fig. 11. Measured antenna patterns for two-dimensional power combining array.

Further, when the oscillator is made in a monolithic fashion, only the drain bias network is required by making use of self-biasing for the FET's, and its network can be simplified by utilizing a coupling line for the power combining.

It is expected that, using the technology demonstrated in this paper, a compact and potentially low-cost quasi-optical power combining array can be realized.

APPENDIX

Antenna Input Impedance

An input impedance of an antenna has a real part and an imaginary part which depend on frequency. The antenna is designed to resonate so that its reactive part is equal to zero. In this case, the design frequency of the passive part of the quasi-optical oscillator is identical with the resonant frequency of the antenna.

Since we chose a slot antenna as a radiator, let us consider the input impedance of the slot suitable for the design of the active antenna. For a slot antenna in a homogeneous space, we can use Booker's formula to relate the input impedance of a slot antenna to that of the complementary dipole antenna. However, in the case of a printed antenna on a dielectric substrate, we must use Booker's formula with a mean dielectric constant, which is approximately valid [10].

$$Z_{\text{slot}} \cdot Z_{\text{dipole}} = \eta_m^2/4$$

where

$$\eta_m = \sqrt{(\mu/\varepsilon_m)}$$
$$\varepsilon_m = (\varepsilon_{air} + \varepsilon_{diel})/2$$

Using this formula, we can convert the problem of the input impedance of the slot antenna into that of the dipole antenna.

For the analysis of the dipole antenna, we can use the two types of integral equations; the Pocklington type and the Hallen type [11]. We used the Pocklington type integral equation, since it is generally used for a numerical calculation. This integral equation is then solved numerically by the point matching technique. In the calculation, 0.25 of the slot width is used as the equivalent radius of the dipole.

However, when the slot width increases, agreement between the experimental resonant slot length and the theoretical resonant length deteriorates. For instance, the theoretical second resonant slot length, L_{sr}, becomes $0.68\lambda_{pc}$ (where λ_{pc} indicates the wavelength used in the calculation of the Pocklington type integral equation), while the experimental resonant slot length, L_{ex}, is almost $1\lambda_s$, when the slot width is $0.081\lambda_s$. Here, let us assume for the circuit analysis that these two resonant slot lengths, L_{sr} and L_{ex}, are identical and the theoretical calculation can explain the experimental status around the second resonant slot length. Under this assumption, the theoretical resonant frequency can be identified with the design frequency of the circuit and, then, characteristics of the quasi-optical circuit can be investigated, including the antenna input impedance. Therefore, a ratio of the second resonant slot length (L_{sr}) to the operating wavelength (λ) can be used as an operating slot length (L_n) to make the theoretical input impedance of the slot antenna meet the impedance of a model of the quasi-optical circuit $(L_n = L_{sr}/\lambda)$. The resistance and the reactance of the input impedance of the slot antenna depending on the operating slot length are shown in Fig. 12. Applying the curve fitting within 0.7 to 1.3 of the operating slot length, we obtained the following relationship

$$R = \mathrm{Re}\{Z_s\} = 10^4.(0.266L_n^4 - 1.027L_n^3 + 1.757L_n^2 - 1.351L_n + 0.401) \quad (1)$$

$$X = \mathrm{Im}\{Z_s\} = 10^2.(-0.982L_n^2 + 3.679L_n - 2.706) \quad (2)$$

In both expressions, the correlation coefficients are 1.0 within this range. Using (1) and (2), the slot is expressed as one of the lumped elements in the equivalent circuit model.

In our circuit, an antenna network consists of a quarter wavelength open-circuit microstrip-to-slot line transition and a slot radiator. A crossing slot in the ground plane works as a series impedance as shown in Fig. 3 [12], the input impedance of this antenna network is calculated as

$$Z_{ANT} = \frac{Z_o}{j\tan\beta L_{qt}} + Z_s$$

Here, Z_o is the characteristic impedance of the quarter wavelength transition and L_{qt} is a physical length of the transition. Z_s is the input impedance of the slot antenna.

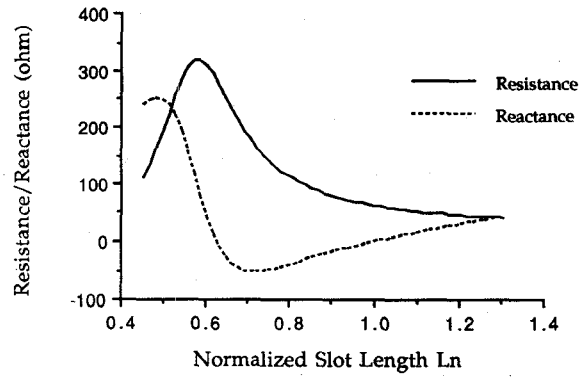

Fig. 12. Slot antenna input impedance.

ACKNOWLEDGMENT

The authors wish to thank Dr. T. Hirota for his helpful suggestions to improve this manuscript.

REFERENCES

[1] T. Itoh, "Active antennas," *Journees In't De Nice Sur Les Antennes,* France, pp. 435–438, Nov. 1990.
[2] J. W. Mink, "Quasi-optical power combining of solid-state millimeter-wave sources," *IEEE Trans. Microwave Theory Tech.,* vol. MTT-34, pp. 273–279, Feb. 1986.
[3] Z. B. Popovic, R. M. Weikle II, M. Kim, and D. B. Rutledge, "A 100-MESFET Planar Grid Oscillator," *IEEE Trans. Microwave Theory Tech.,* vol. 39, pp. 193–200, Feb. 1991.
[4] J. Birkeland and T. Itoh, "A 16 element quasi-optical FET oscillator power combining array with external injection locking," *IEEE Trans. Microwave Theory Tech.,* vol. 40, pp. 475–481, Mar. 1992.
[5] R. A. York and R. C. Compton, "Quasi-optical power combining using mutually synchronized oscillator arrays," *IEEE Trans. Microwave Theory Tech.,* vol. 39, pp. 1000–1009, June 1991.
[6] S. Kawasaki and T. Itoh, "40 GHz quasi-optical second harmonic spatial power combiner using FETs and slots," in *1992 IEEE MTT-S Int. Microwave Symp. Dig.,* Albuquerque, NM, June 1992, pp. 1543–1546.
[7] ——,"6-element periodic and nonperiodic linear arrays for quasi-optical spatial power combiner," *1992 Joint Symposia, URSI Radio Science Meeting,* Chicago, IL, July 1992, p. 394.
[8] ——, "A layered negative resistance amplifier and oscillator using a FET and a slot antenna," *1991 IEEE MTT-S Int. Microwave Symp. Dig.,* vol. 3, Boston, MA, June 1991, pp. 1261–1264.
[9] K. D. Stephan and T. Itoh, "Recent efforts on planar components for active quasi-optical applications," in *1990 IEEE MTT-S Int. Microwave Symp. Dig.,* vol. 3, Dallas, TX, May 1990, pp. 1205–1208.
[10] D. B. Rutledge, D. P. Neikirk, and D. P. Kasilingam, "Integrated-circuit antenna," in *Infrared and Millimeter Waves,* vol. 10, K. J. Button, Ed. New York: Academic Press, 1983, pp. 1–87.
[11] C. A. Balanis, *Antenna Theory.* New York: Wiley, 1982, pp. 304–307.
[12] D. M. Pozar, "A reciprocity method of analysis for printed slot and slot-coupled microstrip antenna," *IEEE Antennas Propagat.,* vol. AP-34, pp. 1439–1446, Dec. 1986.

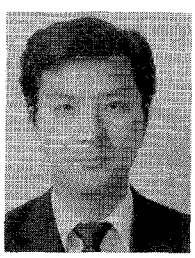

Shigeo Kawasaki received the B.S. and M.S. degrees in electrical engineering from Waseda University at 1979 and 1981, respectively and the Ph.D. degree in electrical engineering from University of California, Los Angeles in 1993.

From April 1981 to October 1989, he joined 3rd Research Center, Technical Research and Development Institute, Japan Defense Agency. In 1990, he was a Research Assistant at The University of Texas at Austin. From January 1991 to March 1993, he was a Graduate Student Researcher at University of California, Los Angeles. His Ph.D. work involved in the quasi-optical power combining arrays using FET's and their optical control.

Tatsuo Itoh (S'69–M'69–SM'74–F'82) for photograph and biography, see this issue, p. 1837.